Available online at www.sciencedirect.com
ScienceDirect
International Journal of Pharmaceutics 344 (2007) 135–142
INTERNATIONAL JOURNAL OF PHARMACEUTICS
www.elsevier.com/locate/ijpharm

Biodistribution of intravenously administered amphiphilic β-cyclodextrin nanospheres

A. Gèze [a,*], L. Tieu Chau [a], L. Choisnard [a], J.-P. Mathieu [b], D. Marti-Batlle [b], L. Riou [b], J.-L. Putaux [c,1], D. Wouessidjewe [a]

[a] *Université Joseph Fourier, UFR de Pharmacie, ICMG FR-2607, DPM UMR UJF/CNRS 5063, BP 53, F-38041 Grenoble Cedex 9, France*
[b] *INSERM E0340, Radiopharmaceutiques Biocliniques, Faculté de Médecine de Grenoble I, Domaine de la Merci, 38700 La Tronche, France*
[c] *Centre de Recherches sur les Macromolécules Végétales (CERMAV-CNRS), BP 53, F-38041 Grenoble Cedex 9, France*

Received 13 February 2007; received in revised form 21 June 2007; accepted 27 June 2007
Available online 5 July 2007

Abstract

Amphiphilic β-cyclodextrin (βCDa) nanospheres (mean diameter 90–110 nm) prepared by the solvent displacement method were developed as a colloidal drug delivery system. In order to survey the fate of these nanoparticles, the amphiphilic β-cyclodextrin was first iodinated by a two-step procedure involving iodination of the primary face followed by an acylation of the secondary face. After radiolabeling of this derivative with ^{125}I, nanospheres made of βCDa/βCDa ^{125}I were formulated. After a single intravenous injection of labeled nanoparticles in mice, the organ distribution was analyzed from 10 min to 6 days. A rapid clearance of ^{125}I-labeled βCDa nanospheres from the blood circulation to the mononuclear phagocyte system was visualized by non-invasive planar imaging study. Radioactivity measurements in organs showed that the nanospheres mainly concentrated in the liver and the spleen where 28 and 24% of the radioactivity per gram of organ was, respectively, found 10 min after injection. At the opposite, the blood activity was low at that time and become negligible thereafter. Finally, the fact that no particular sign of toxicity is observed in injected animals should be emphasized since it is the first report on intravenous administration of βCDa nanoparticles.

Keywords: Amphiphilic β-cyclodextrin; Nanosphere suspension; Cryo-TEM; Radiolabeling; γ-Scintigraphy; In vivo tissue distribution

1. Introduction

The last 20 years have witnessed an explosion in research on the development of new drug delivery systems. One of the strategy concerns the use of colloidal systems. Among these colloidal carriers, liposomes which consist of one or more phospholipid bilayer surrounding an aqueous core and biodegradable polymer-based nanoparticles have been widely investigated. Some of them have found pharmaceutical marketed application while other systems are still under clinical trials (Lasic, 1998; Barrat, 2000; Allen and Cullis, 2004; Couvreur and Vauthier, 2006). In this context, a new generation of nanoparticles composed of chemically modified cyclodextrins, a non polymeric material, has been introduced in the 1990s (Skiba et al., 1992a,b; Wouessidjewe et al., 1996). Cyclodextrins are enzymatic degradation products of starch consisting of 6 (αCD), 7 (βCD) or 8 (γCD) glucopyranose units linked by α(1–4) glycosidic bonds and commercially available (Biwer et al., 2002). Owing to their particular structure, which consists of a hydrophilic external surface and a more hydrophobic cavity lined with protons, cyclodextrins are capable of forming inclusion complexes with a variety of guest molecules. In this context, they have been widely used as pharmaceutical excipients (Davis and Brewster, 2004) to formulate drugs with poor bioavailability (poorly soluble, unstable or severe side-effects associated drugs). Numerous chemical modifications have been carried out on cyclodextrins by grafting substituents to different positions (primary face, secondary face or both faces) to obtain non ionic or cationic derivatives able to form supramolecular aggregates in the form of nanostructures used for pharmaceutical applications (Lemos-Senna et al., 1998; Duchêne et al., 1999; Auzély-Velty et al., 2000; Dubes et al., 2001; Mazzaglia et al., 2002; Memisoglu et al., 2002; Skiba et al., 2002; Cryan et al., 2004; Péroche et al., 2005). Among the

* Corresponding author. Tel.: +33 4 76 63 53 01; fax: +33 4 76 63 53 22.
E-mail address: annabelle.geze@ujf-grenoble.fr (A. Gèze).
[1] Affiliated with Université Joseph Fourier and Member of the Institut de Chimie Moléculaire de Grenoble, France.

0378-5173/$ – see front matter © 2007 Elsevier B.V. All rights reserved.
doi:10.1016/j.ijpharm.2007.06.050

modifications realized, a series of molecules have been obtained by grafting fatty acids of different chain lengths on the hydroxyl groups of the secondary face involving either a chemical (Zhang et al., 1991) or more recently an enzymatic way (Perdersen et al., 2005). The ability of these amphiphilic cyclodextrin derivatives to self-assemble into submicronic systems have been previously demonstrated (Lemos-Senna et al., 1998; Choisnard et al., 2006). This family of cyclodextrin derivatives offer a wide range of particle morphologies, like matrix (nanospheres), reservoir (nanocapsules) or rather lamellar structures (Lemos-Senna et al., 1998; Gèze et al., 2002; Memisoglu-Bilensoy et al., 2005; Choisnard et al., 2005, 2006). Moreover, these particular architectures made of organized CD molecular entities may offer the opportunity to associate drug molecules at different levels within the nanostructure, i.e. surface adsorption, matrix entrapment, or interaction with the cavity of cyclodextrins. These features may be of interest in terms of protection and drug release. Also, the influence of CDa nanoparticles on drug absorption was recently reported (Rival et al., 2006). The size range of cyclodextrin-based nanoparticles is compatible with an intravenous administration. his route of administration has not been investigated yet with "skirt shaped" type amphiphilic β-cyclodextrin. In order to follow the nanoparticle biodistribution, the amphiphilic derivative modified on the secondary face was radiolabeled. The study was monitored by planar scintigraphic imaging and activity measurements after tissue dissection. For this purpose, iodination of the primary face of amphiphilic βCD was performed. This paper reports the synthesis of ^{125}I-radiolabeled compound, the formulation of nanoparticles and the in vivo tissue distribution studies.

2. Materials and methods

2.1. Materials

βCD was kindly donated by Roquette Frères (Lestrem, France) and was used after drying at 80 °C for 48 h under reduced pressure (1 mbar) in the presence of P_2O_5. Triphenylphosphine (99%), hexanoyle chloride (99%) and 2,4-dimethylaminopyridine (99%) were purchased from Sigma–Aldrich. Iodine (99.8%) was obtained from Fluka. Pyridine was distilled and stored under molecular sieve before use. $Na^{125}I$ (37 MBq mL^{-1}) was from Life and Analytical Science (USA) and the ion exchange resin column AG 1-X8 chloride (200,400 mesh) of analytical grade was obtained from BIO-RAD. Water was freshly distilled in our laboratory. All the other chemicals were of analytical grade and used as received.

2.2. Per-(6-iodo-2,3-di-O-hexanoyl)-β-cyclodextrin (βCDaI) synthesis

βCDa was synthesized in three steps as described elsewhere (Zhang et al., 1991): protection of primary hydroxyl groups, acylation of secondary hydroxyl groups and then deprotection of primary hydroxyl groups. βCDaI was synthesized in two steps as below: (1) iodination of primary hydroxyl groups localized on C6 position of β-cyclodextrin (βCD) leads to per-6-iodo-β-cyclodextrin (βCDI) (Ashton et al., 1996) and (2) acylation of secondary hydroxyl groups localized on C2 and C3 of βCDI using hexanoyl chains:

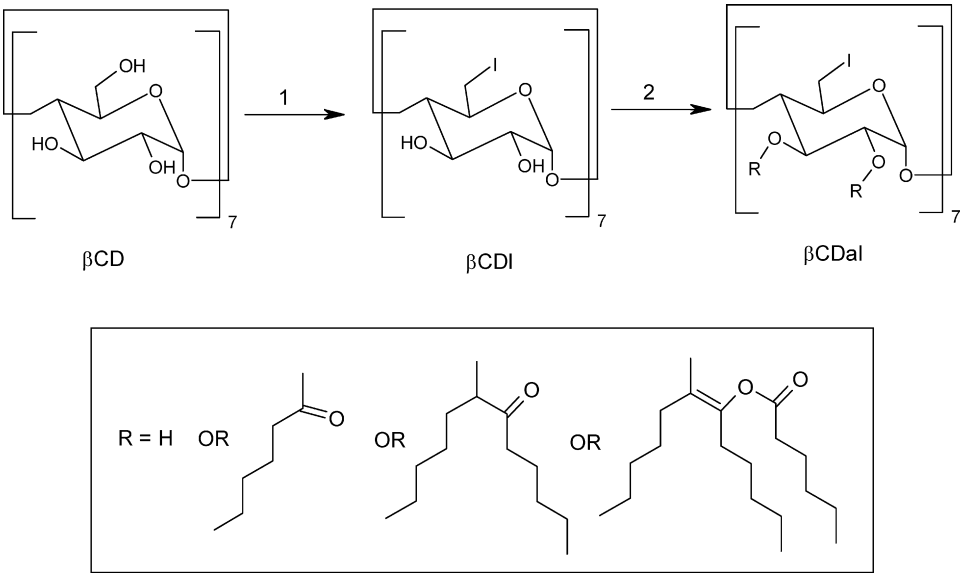

βCD βCDI βCDaI

(**1**) triphenylphosphine (40.1 g, 153 mmol) was dissolved under agitation in dry *N*,*N*-dimethylformamide (160 mL) at room temperature. Then, I_2 (40.5 g, 160 mmol) was added over 10 min to this solution which was thermostated to 50 °C. The temperature of the stirred solution was raised to 70 °C and dried βCD (1 g, 0.88 mmol) was added under an atmosphere of N_2 for 18 h. pH was adjusted to 9–10 by the addition of NaOMe in methanol (3 M, 30 mL) with external cooling. The solution was stirred for 30 min at room temperature. The product was precipitated in ice-cooled water and poured in methanol (800 mL). Precipitate was filtered, washed by methanol, and extracted by Soxhlet extractor with methanol for 20 h. The product was recovered as βCDI (1.6 g, 95%): NMR (Avance 400 MHz, Bruker,); ^{1}HNMR δ_H (DMSO) 6.06 (d, 1H, OH-2); 5.94 (s, 1H, OH-3); 4.97 (s, 1H, H-1); 3.2–3.9 (m, 6H, H-3,

H-2, H-4, H-5, 2H-6); ^{13}CNMR (DMSO): δ 102.6 (C1); 86.4 (C-4); 72.4 (C-3); 71.4 (C-5); 9.9 (CH_2-I); Mass spectrometry MALDI/TOF ($CHCl_3$/MeOH; 90/10): $m/z = 1926$ ($[M + Na]^+$); mp: 245–250 °C.

(**2**) Hexanoyl chloride (6 mL, 45 mmol) was added to a stirred solution of βCDI (1.9 g, 1 mmol) and 2, 4-dimethylaminopyridine (6 g, 49 mmol) in anhydrous pyridine (40 mL). The mixture was heated at 70 °C for 48 h then cooled to room temperature and poured into a large volume of ice-cooled water. The aqueous phase was removed by settling and the residue taken up into dichloromethane. After washing with dilute sulphuric acid, water and aqueous sodium hydrogen carbonate, the organic phase was dried (Na_2SO_4) and concentrated to a residue which was submitted to column chromatography using chloroform/cyclohexane (6/4) as mobile phase.

2.3. Radiolabeling of βCDaI

The isotopic exchange with $^{125}I^-$ was carried out by mixing solutions (39:61) of βCDaI (5 mg) and NaI (4 μg/mL) in anhydrous acetone to obtain a volume of 1 mL, by adding $Na^{125}I$ solution (37 MBq), then by heating the final solution at around 105 °C during 2.5 hours. Unbound $^{125}I^-$ and I^- were eliminated by ion exchange resin column (AG 1-X8 chloride form). $^{125}I^-$ exchange yield was determined using a dose calibrator (Capintec CRC-15R, USA).

2.4. Nanoparticle preparation

Non radiolabeled nanoparticles of different w/w βCDa/βCDaI mixtures (100/0, 50/50, 0/100) were prepared by the solvent displacement method (Fessi et al., 1992). Briefly, the amphiphilic material was dissolved in anhydrous acetone in order to obtain a concentration of 1 mg/mL. This solution was then incorporated into an equal volume of distilled water under magnetic stirring (500 rpm). The distilled water was replaced by a 5% glucose solution (Lavoisier, France) to ensure isotonicity for in vivo studies. Nanoparticles were formed spontaneously and organic solvent was then removed under reduced pressure and the suspension was concentrated until a final volume of 5 mL. The aqueous suspension was filtered through 0.8 μm (Millex AA, Millipore, France). Radiolabeled nanoparticles were made with a mixture of fresh radiolabeled βCDa ^{125}I and non-iodinated βCDa (1:1) and prepared in a similar way using 5% aqueous glucose solution. In order to verify the stability in a physiological medium, the different compositions of nanosphere suspension (2.5 mL) were incubated in 2.5 mL foetal bovine serum during several days and were visually observed (looking for sedimentation).

2.5. Stability of radioactive iodine labeling

The evaluation of ^{125}I-labeled βCDa nanospheres stability was performed as follows. An anesthetized mouse was injected with 50 μL of heparin in phosphate-buffered saline (250 IU/mL) prior to being submitted to chest opening and intracardiac blood withdrawal (∼0.5 mL). Blood centrifugation was performed immediately (5 min, 4,000 rpm) and the serum (∼0.3 mL) was used for ^{125}I-labeled βCDa nanospheres incubation at 37 °C. After 5 min, 60 min, and 60 h of incubation, an aliquot was analyzed using thin layer chromatography (TLC) with an RP-18 F 254 plate (Merck) and NaCl 0.9% as the eluent. TLC profiles were compared with that obtained immediately following nanosphere radiolabeling. A Berthold- LB 2842 plate reader was used for TLC plate analysis.

2.6. Size and zeta potential measurements

A Zetasizer 3000 instrument (10 mW HeNe laser at 632.8 nm) with a K7132 correlator was used at the fixed angle of 90° and at 25 ± 0.1 °C for size analysis and zeta potential determination (Malvern Instruments, Orsay, France). The Z average hydrodynamic diameter Dh (Z average mean) and polydispersity index PI were calculated in intensity using the Cumulant analysis mode. Dh values was derived from the measured translational diffusion coefficient of the particles moving under Brownian motion. The values of merit for size analysis varied from 60 to 70%. Zeta potential values were evaluated by laser Doppler anemometry. In both determinations, non radiolabeled colloidal suspensions were analyzed following appropriate dilution with phosphate buffer pH 7.3 (10^{-3} M).

2.7. Cryo-transmission electron microscopy (cryo-TEM)

Thin vitrified films of non radiolabeled βCDa nanoparticle suspensions were prepared as described elsewhere (Gèze et al., 2004). Droplets of 0.1% (w/v) suspensions were deposited on 'lacey' carbon films. After blotting the liquid in excess with filter paper, the grid was quench-frozen into liquefied ethane. The specimens were then mounted in a Gatan 626 cryo-holder, transferred into a Philips CM200 'Cryo' microscope and observed at low temperature (−180 °C), under reduced illumination, at an accelerating voltage of 80 kV. Images were recorded on Kodak SO163 films.

2.8. Evaluation of the nanoparticle biodistribution by in vivo imaging

All the experiments described in the present study were approved by the Animal Care and Use Committee use of the Centre de Recherche et Service de Santé des Armées (CRSSA-authorization #2004/25.0) and the experiments were performed by an authorized individual (D. Marti-Battle, authorization #38 03 21). The βCDa ^{125}I nanoparticle suspension was injected in the tail vein of four OF1 male mice (50 μL–2.4 MBq) anesthetized with an intraperitoneal injection of a mixture of ketamine (10%, w/v, to 75 mg/kg)/xylazine (2% g/v to 15 mg/kg) (1:1) (total injected volume ∼30 μL). Sixty (60)-min non-invasive whole body planar imaging using a small animal dedicated gamma camera (gamma-imager, Biospace Mesures, Paris, France) was started immediately following tracer injection. One animal was re-imaged 6 days after injection. Regions of interest (ROIs) were drawn on the liver and spleen on

images performed at 1, 5, 15, 30, 60 min following tracer injection ($n=4$) as well as at day 6 ($n=1$). ROI image quantification yielded liver and spleen activity in counts/min/mm^2 (CPM/mm^2) which were then normalized to the injected dose in MBq/kg of body weight, yielding results expression in [CPM/mm^2]/[MBq/kg].

2.9. Evaluation of the nanoparticle biodistribution by post-mortem assessment of organ activity

36 health Swiss male mice (25–30 g) (Janvier Society, France) were divided into six groups.

Animals were used in experiments after 24–48 h stabulation period. Whenever necessary over the course of the experiments, they were housed in stainless steel cages at room temperature and had free access to drinking water and food. Bolus intravenous (IV) injections (BD^{TM} Micro-Fin syringe, insulin type (29 G)) of 50 μL of a freshly prepared βCDa ^{125}I nanosphere suspension corresponding to a radioactivity of 11–33 MBq were given via the tail vein. At 10 min, 1 h, 4 h, 24 h, 48 h, and 6 days after injection, blood samples were collected by cardiac puncture. After blood collection, the animals were euthanized by cervical dislocation. Samples from the liver, lungs, kidneys, spleen, heart, brain, stomach, intestine, and skin were obtained, quickly rinsed and weighed. The whole tail was also obtained to ensure the successfulness of the intravenous injection. The activity in the thyroid and in the urine was checked as well in four animals 60 min after injection and in one animal at day 6. Tissue radioactivity was measured using a gamma-well counter (COBRA TM II Auto-Gamma, Packard instrument SA.). Following decay correction, the organ activity of the nanoparticles was expressed as percentage of the injected dose per gram of wet weight (% ID/g).

2.10. Statistical analysis

Statistical analysis of data was performed using a one-way ANOVA. A value of $p<0.05$ for the comparisons was considered to represent a significant difference between groups. Post hoc pairwise multiple comparisons were conducted using the Holm-Sidak method to identify the groups that differed from the others (overall significant level = 0.05). All the tests were performed using SigmaStat statistics software.

3. Results and discussion

3.1. βCDa, βCDaI synthesis, material labeling

βCDa was obtained as a mixture of overacylated products as a result of the large excess of DMAP used in the acylation step, which favors condensation of hexanoyl chains between each other in the mixture (Höfle et al., 1978; Lesieur et al., 2000; Dubes et al., 2001). The iodinated amphiphilic product was supposed to be a mixture of differently acylated species, as the parent βCDa. The hydroxyl groups of the primary face was totally iodinated as revealed by ^{1}HNMR and mass spectrum data of βCDI. Isotopic exchange yield of βCDa ^{125}I was close to 80%. The absence of free iodine ions in the product was confirmed before formulation by thin layer chromatography (results not shown). Since labeling conditions implies the use of acetone, the radioisotope was introduced in the amphiphilic βCD before the formulation of the nanoparticles.

3.2. Nanoparticle formulation and characterization

The βCDa/βCDa ^{125}I ratio (1:1) freshly radiolabeled used to prepare the nanoparticles was chosen in order to obtain a labeled suspension whose characteristics were close to the original material to study. The presence of βCDaI, while keeping its ability to self-organize, slightly increased mean size particles (from 90 nm for βCDa to 110 nm for βCDa/βCDa ^{125}I with polydispersity indexes of 0.06 and 0.07) as illustrated in Fig. 1. The size distributions were partly superimposed and were thus in the same range of size. The βCDa/βCDa ^{125}I-based-nanoparticles presented a monodisperse distribution meaning that the iodinated and non-iodinated derivatives co-nanoprecipitated, which was a prerequisite for the study in order to evaluate the fate of the whole population of nanoparticles. The size results are in accordance with the data obtained from cryo-TEM images, where the two suspensions are shown in Fig. 2. Individual spherical βCDa (Fig. 2a) and βCDa/βCDaI (Fig. 2b and c) nanoparticles are observed embedded in vitreous ice. No aggregation of the particles was observed. A size-distribution histogram of the βCDa suspension was determined by measuring the diameter of 400 nanospheres from the cryo-TEM images (Fig. 2d). A mean number diameter of 76 nm was found. This result is in accordance with the one obtained by DLS (90 nm). The slight deviation between both methods has already been observed and discussed elsewhere (Gèze et al., 2004). As seen in Fig. 2c, a darker layer at the periphery of the βCDa/βCDaI nanoparticles is often observed. As an imaging artefact from defocusing was ruled out, the darker periphery of the nanospheres (Fig. 2b-c) suggested that some heavier iodine atoms might have accumulated on the surface of the nanospheres. This suggestion is in accordance with the higher negative zeta potential characterizing the βCDaI-based nanoparticles (−45 mV), the iodine being

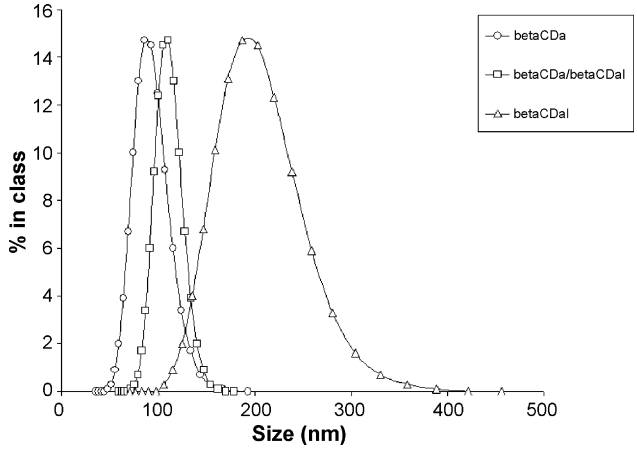

Fig. 1. Size distribution of βCDa, βCDaI and βCDa/βCDaI-based nanoparticles, as measured using photon correlation spectroscopy.

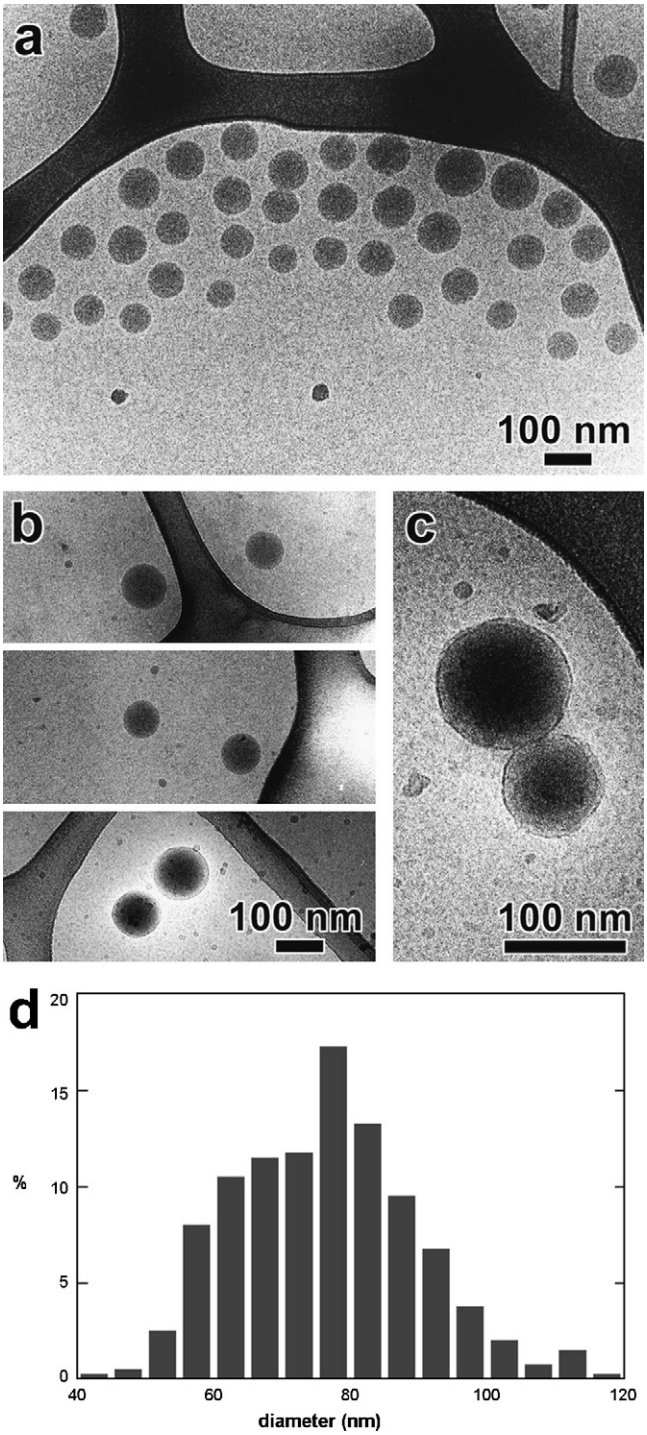

Fig. 2. (a–c) Cryo-TEM images of amphiphilic β-cyclodextrin nanospheres: (a) βCDa; (b and c) 50/50 βCDa/βCDaI; (d) size-distribution histogram of the βCDa nanospheres, as measured from the cryo-TEM images.

an electronegative atom. One can note that the zeta potential values characterizing the βCDa (−29 mV) and βCDa/βCDaI (−32 mV) nanoparticles are similar. Moreover, the cryo-TEM observations show that the presence of iodine atoms in the primary face of the βCD derivatives did not modify the overall morphology and the size range of the nanoparticles. For all these precited reasons, it was stated that the characteristics of the βCDa/βCDaI mixed suspension were comparable to the one of βCDa nanospheres and was suitable for in vivo studies.

3.3. Nanoparticle distribution study

The results of the evaluation of nanoparticle distribution as obtained by non-invasive planar scintigraphic imaging in mice showed that the tracer activity was mainly localized in the abdomen area of the animals early following iv administration (Fig. 3). The liver and spleen represented the main sites of ^{125}I-labeled βCDa nanospheres uptake as early as 1 min post-injection and tracer activity remained stable in those organs as late as 6 days following injection. One can note that the whole body imaging did not show any iodine accumulation in the thyroid, as confirmed by the low activity level measured in this organ after tissue dissection (0.9 ± 0.4% ID/g) 60 min following the injection. This low level was maintained at day 6 (0.8% ID/g). The absence of such accumulation in the thyroid is in accordance with the low radioactivity found in the stomach and intestine (Fig. 4). In parallel, the stability of the radioactive iodine labeling of the nanoparticles has been controlled in biological medium by incubating the radiolabeled suspension with mouse serum at 37 °C for various time periods. The results indicated that ^{125}I-labeled βCDa nanospheres stability was excellent even following a 60 h incubation period, thereby confirming biodistribution results, which indicated neither thyroid nor stomach accumulation of ^{125}I over time. It is noteworthy to point out that the presence of radioactivity does not necessarily imply the presence of intact nanospheres. However, the rapidity of the uptake by the liver and spleen, as shown in Fig. 4, and the good labeling stability suggests that intact particles are being followed. Blood activity was low as early as 10 min following injection and was negligible thereafter indicating that the βCDa-based nanospheres have a very short circulation time in the vascular compartment. Also, ten minutes after injection, 28% of radioactivity per gram of organ was found in the liver and 24% in the spleen (Fig. 4b). Low levels of radioactivity could be detected in the heart, lungs and kidneys and the radioactivity was not detectable neither in the brain nor skin. The data indicated that nanospheres were rapidly cleared from the blood compartment to localize to the mononuclear phagocyte system, particularly to liver and spleen macrophages after injection via the intravenous route in mice. The in vivo behavior of the nanoparticles made of βCDa is similar to those widely reported in the literature for various colloidal systems (Rolland et al., 1989; De Keyser et al., 1991; Bazile et al., 1995; Moghimi et al., 2001; Couvreur and Vauthier, 2006). It partly reflects the localization of the fixed macrophages of the mononuclear phagocyte system (MPS) in the liver and in the spleen which participate to a major degree in the clearance of particles from the blood. The hepato-splenic distribution also refers to the histological structure of vascular endothelium of these tissues. Indeed, it is known that colloids can escape from the circulation through the open fenestrae of the capillaries of the sinus endothelium of the liver (Moghimi et al., 2001). Radioactivity remained in liver and spleen for 6 days. The liver activity significantly decreased between 1 h and 6 days following injection ($p = 0.016$) whereas

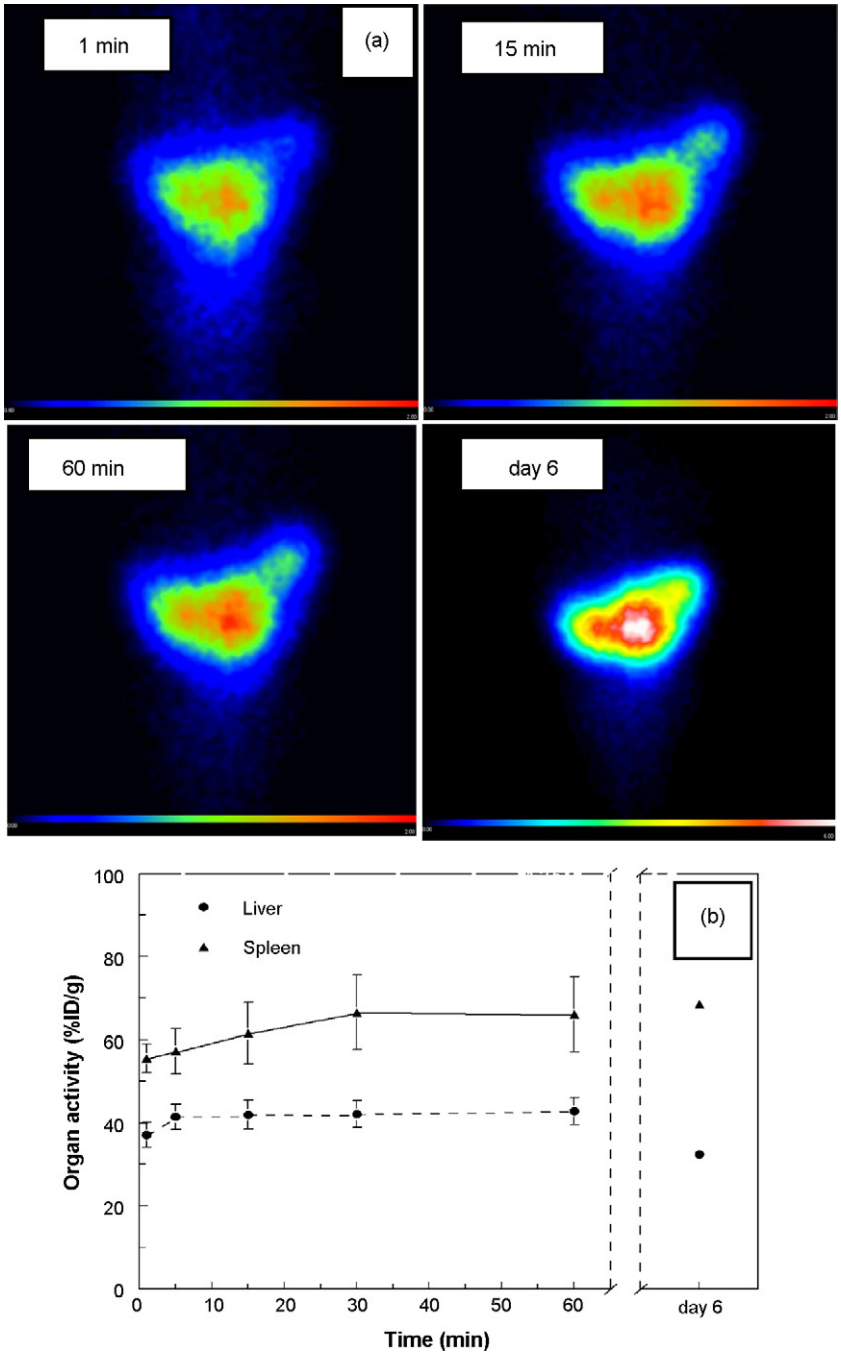

Fig. 3. (a) Scintigraphic planar images from a mice at times 1 min, 15 min, 60 min and day 6 following the intravenous injection of ^{125}I-labeled βCDa nanospheres. (b) Liver and spleen activity of ^{125}I-labeled βCDa nanospheres over time from non invasive in vivo imaging ($n = 4$ from 1 to 60 min/$n = 1$ at day 6).

there was no statistical difference in the spleen radioactivity mean values ($p = 0.266$). The significant reduction in the liver activity between 1 h and 6 days following injection may be due to a partial elimination or biodegradation of nanoparticles since intact particles are retained by fixed macrophages and partially by Kupffer cells in this organ (Korsakov and Bechthold, 2000). During this period, the animals did not present any visible symptoms of toxicity related to the injection of the radiolabeled nanoparticles. This lack of toxicity has to be emphasized since this is the first report on βCDa nanoparticles intravenous administration. In another part, the βCDa nanosuspensions have demonstrated long term shelf stability over periods of 3 years in distilled water without the use of a surfactant (Gèze et al., 2004). This physical stability observed in water seems to be maintained in vivo. Indeed, in our study, the low lung activity observed may be attributable to the lack of mechanical filtration by the capillary bed due to the size of nanoparticles smaller than 200 nm and their negative zeta potential charge (near −30 mV), indicating that most likely no nanosphere flocculation occurs in the blood (Korsakov and Bechthold, 2000). This behavior is in accordance with the absence of flocculation of the nanoparticle suspensions when in contact with foetal bovine serum, show-

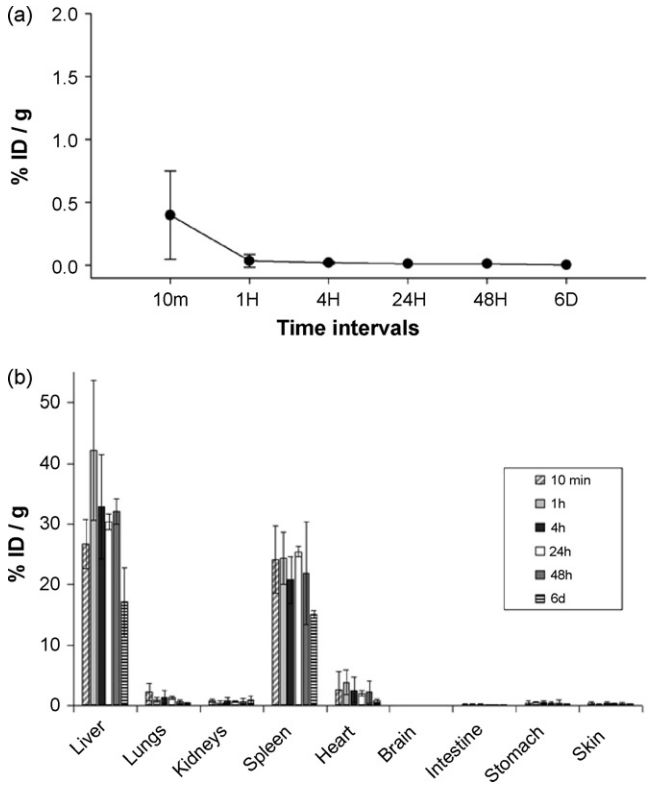

Fig. 4. (a) Blood kinetics of ^{125}I-labeled βCDa nanoparticles; (b) Organ distribution of ^{125}I-labeled βCDa nanoparticles after intravenous administration to mice ($n = 3$–5). Values are expressed as percent of the injected dose per gram of organ, mean ± (S.D.).

ing the potential physical stability of the nanosuspensions in a physiological complex medium. Consequently, the use of a stabilizing agent was not required for the in vivo studies. This represents an advantage with respect to the increased cytotoxicity observed by Memisoglu-Bilensoy et al. (2006) with similar βCDa nanoparticles stabilized by a surfactant. These amphiphilic βCD derivatives have also been shown to be non-hemolytic in injectable nanosphere form by the same authors (Memisoglu et al., 2003).

In conclusion, the use of a stable ^{125}I label allowed for the first time an extended follow up of the biodistribution in mice of amphiphilic βCD nanoparticles. As the other uncoated particulate nanocarriers, the nanospheres of βCDa were rapidly cleared from blood stream and accumulated in the liver and spleen, suggesting their potential use in passive targeting of some hepatic diseases. Despite the latest application, further chemical modifications of βCDa and formulation studies are needed to achieve long-circulating and site-specific targeted nanoparticles of amphiphilic βCD. At the same time, our work showed that nanoaggregates made of βCDa were rather well tolerated by the animals, in the limits of the monitored period, since no apparent signs of toxicity nor death were observed. Further histological studies would be helpful to evaluate the local effects of βCDa in the different tissues. Besides, amphiphilic βCD nanoparticles possess other advantages: they keep CD host cavity for drug complexation, they provide a variety of supramolecular architectures which offer opportunity of designing nanocarriers able to protect and release the drug candidate with different pathways. Finally, these preliminary results on the in vivo fate of βCDa-based nanoparticles are encouraging and must be considered as the basis of further extensive studies.

References

Allen, T.M., Cullis, P.R., 2004. Drug delivery systems: entering the mainstream. Science 303, 1818–1822.

Ashton, P.R., Königer, R., Stoddart, J.F., Alker, D., Harding, V.D., 1996. Aminoacid derivative of β-cyclodextrin. J. Org. Chem. 61, 903–908.

Auzély-Velty, R., Djedaïni-Pilard, F., Désert, S., Perly, B., Zemb, Th., 2000. Micellization of hydrophobically modified cyclodextrins. 1 Micellar Structure. Langmuir 16, 3727–3734.

Barrat, G.-M., 2000. Therapeutic applications of colloidal drug carriers. Pharm. Sci. Technol. Today 3, 163–169.

Bazile, D., Prud'Homme, C., Bassoulet, M.T., Marlard, M., Spenlehauer, G., Veillard, M., 1995. Stealth Me.PEG-PLA nanoparticles avoid uptake by the mononuclear phagocytes system. J. Pharm. Sci. 84, 493–497.

Biwer, A., Antranikian, G., Heinzle, E., 2002. Enzymatic production of cyclodextrins. Appl. Microbiol. Biotechnol. 59, 609–617.

Choisnard, L., Gèze, A., Bigan, M., Putaux, J.-L., Wouessidjewe, D., 2005. Efficient size control of amphiphilic cyclodextrin nanoparticles through a statistical mixture design methodology. J. Pharm. Pharmaceut. Sci. 8, 593–600.

Choisnard, L., Gèze, A., Putaux, J.-L., Wong, Y.S., Wouessidjewe, D., 2006. Nanoparticles of β-cyclodextrin esters obtained by self-assembling of biotransesterified β-cyclodextrins. Biomacromolecules 7, 515–520.

Couvreur, P., Vauthier, C., 2006. Nanotechnology: intelligent design to treat complex disease. Pharm. Res. 23, 1417–1450.

Cryan, S.A., Donohue, R., Ravoo, B.J., Darcy, R., O'Driscoll, C.M., 2004. Cationic cyclodextrin amphiphiles as gene delivery vectors. J. Drug Del. Sci. Techn. 14, 57–62.

Davis, M.E., Brewster, M.E., 2004. Cyclodextrin-based pharmaceutics: past, present and future. Nat. Rev. Drug Discov. 3, 1023–1035.

De Keyser, J.-L., Poupaert, J.H., Dumont, P., 1991. Poly(diethyl methylidenemalonate) nanoparticles as a potential drug carrier: preparation, distribution and elimination after intravenous and peroral administration to mice. J. Pharm. Sci. 80, 67–70.

Dubes, A., Bouchu, D., Lamartine, R., Parrot-Lopez, H., 2001. An efficient regio-specific synthetic route to multiply substituted acyl-sulphated β-cyclodextrins. Carbohyd. Res. 42, 9147–9151.

Duchêne, D., Ponchel, G., Wouessidjewe, D., 1999. Cyclodextrins in targeting application to nanoparticles. Adv. Drug Del. Rev. 36, 29–40.

Fessi, H., Devissaguet, J.P., Puisieux, F., Thies, C., 1992. Process for the preparation of dispersible colloidal systems of a substance in the form of nanoparticles. US Patent 5,118,528.

Gèze, A., Aous, S., Baussanne, I., Putaux, J.-L., Defaye, J., Wouessidjewe, D., 2002. Influence of chemical structure of amphiphilic β-cyclodextrins on their ability to form stable nanoparticles. Int. J. Pharm. 242, 301–305.

Gèze, A., Putaux, J.-L., Choisnard, L., Jéhan, P., Wouessidjewe, D., 2004. Long-term shelf stability of amphiphilic β-cyclodextrin nanosphere suspensions monitored by dynamic light scattering and cryo-transmission electron microscopy. J. Microencapsul. 21, 607–613.

Höfle, G., Steglich, W., Vorbrüggen, H., 1978. 4-Dialkylaminopyridines as highly active acylation catalysts. Angew. Chem. Int. Ed. Engl. 17, 569–583.

Korsakov, M.V., Bechthold, F., 2000. Nanoparticles in nuclear medicine. Radiochemistry 42, 308–324.

Lasic, D.D., 1998. Novel applications of liposomes. Trends Biotechnol. 16, 307–321.

Lemos-Senna, E., Wouessidjewe, D., Duchêne, D., Lesieur, S., 1998. Amphiphilic cyclodextrin nanospheres: particle solubilization and reconstitution by the action of a non-ionic detergent. Col. Surf. B: Biointerfaces 10, 291–301.

Lesieur, S., Charon, D., Lesieur, P., Ringard-Lefebvre, C., Muguet, V., Duchêne, D., Wouessidjewe, D., 2000. Phase behaviour of fully hydrated DMPC-amphiphilic cyclodextrin systems. Chem. Phys. Lipids 106, 127–144.

Mazzaglia, A., Ravoo, B.J., Darcy, R., Gambadauro, P., Mallamace, F., 2002. Aggregation in water of nonionic amphiphilic cyclodextrins with short hydrophobic substituents. Langmuir 18, 1945–1948.

Memisoglu, E., Bochot, A., Sen, M., Charon, D., Duchêne, D., Hincal, A.A., 2002. Amphiphilic β-cyclodextrins modified on the primary face: synthesis, characterization, and evaluation of their potential as novel excipient in the preparation of nanocapsules. J. Pharm. Sci. 91, 1214–1224.

Memisoglu, E., Bochot, A., Ozalp, M., Sen, M., Duchêne, D., Hincal, A.A., 2003. Direct formation of nanospheres from amphiphilic β-cyclodextrin inclusion complexes. Pharm. Res. 20, 117–125.

Memisoglu-Bilensoy, E., Vural, I., Bochot, A., Rendir, J.-M., Duchêne, D., Hincal, A.A., 2005. Tamoxifen citrate loaded amphiphilic cyclodextrin nanoaprticles: In Vitro characterization and cytotoxicity. J. Control. Release 104, 489–496.

Memisoglu-Bilensoy, E., Dogan, A.L., Hincal, A.A., 2006. Cytotoxic evaluation of injectable cyclodextrin nanoparticles. J. Pharm. Pharmacol. 58, 585–589.

Moghimi, S.M., Hunter, A.C., Murray, J.-C., 2001. Long-circulating and target-specific nanoparticles: theory and practice. Pharmacol. Rev. 53, 283–318.

Perdersen, N.R., Kristensen, J.B., Bauw, G., Ravoo, B.J., Darcy, R., Larsen, K.L., Pedersen, L.H., 2005. Thermolysin catalyses the synthesis of cyclodextrin esters in DMSO. Tetrahedron Asymm. 16, 615–622.

Péroche, S., Dégobert, G., Putaux, J.-L., Blanchin, M.G., Fessi, H., Parrot-Lopez, H., 2005. Synthesis and characterization of novel nanospheres made from amphiphilic perfluoroalkylthio-β-cyclodextrins. Eur. J. Pharm. Biopharm. 60, 123–131.

Rival, D., Terry, N., Bonnet, S., Sohm, B., Perrier, E., Coleman, A., 2006. Nanosized particles based on beta-cyclodextrin esters. SÖFW-J. 132, 54–62.

Rolland, A., Collet, B., Le Verge, R., Toujas, L., 1989. Blood clearance and organ distribution of intravenously administered polymethacrylic nanoparticles in mice. J. Pharm. Sci. 78, 481–484.

Skiba, M., Skiba-Lahiani, M., Arnaud, P., 2002. Design of nanocapsules based on novel fluorophilic cyclodextrin derivatives and their potential role in oxygen delivery. J. Incl. Phenom. Macroc. Chem. 44, 151–154.

Skiba, M., Wouessidjewe, D., Fessi, H., Devissaguet, J.P., Duchêne, D., Puisieux, F., 1992a. Préparation et utilisation de nouveaux systèmes colloïdaux dispersibles à base de cyclodextrines, sous forme de nanosphères. French Patent 9207287.

Skiba, M., Wouessidjewe, D., Fessi, H., Devissaguet, J.P., Duchêne, D., Puisieux, F., 1992b. Préparation et utilisation de nouveaux systèmes colloïdaux dispersibles à base de cyclodextrines, sous forme de nanocapsules. French Patent 9207285.

Wouessidjewe, D., Skiba, M., Leroy-Lechat, F., Lemos-Senna, E., Puisieux, F., Duchêne, D., 1996. A new concept in drug delivery based on "skirt-shaped cyclodextrin aggregates" Present state and future prospects. STP Pharma Sci. 6, 21–28.

Zhang, P., Ling, C.C., Coleman, A.W., Parrot-Lopez, H., Galons, H., 1991. Formation of amphiphilic cyclodextrin via hydrophobic esterification at the secondary hydroxyl face. Tetrahedron Lett. 32, 2769–2770.